Biosensors and Bioelectronics 129 (2019) 24–28

Contents lists available at ScienceDirect

Biosensors and Bioelectronics

journal homepage: www.elsevier.com/locate/bios

Raman tracking the activity of urease in saliva for healthcare

Sen Hu, Yun Gao, Yiping Wu*, Xiaoyu Guo, Ye Ying, Ying Wen, Haifeng Yang*

The Education Ministry Key Lab of Resource Chemistry, Shanghai Key Laboratory of Rare Earth Functional Materials, Shanghai Municipal Education Committee Key Laboratory of Molecular Imaging Probes and Sensors, College of Chemistry and Materials Science, Shanghai Normal University, Shanghai 200234, China

ARTICLE INFO

Keywords:
Urease activity
Urea
Surface-enhanced Raman scattering
Healthcare

ABSTRACT

The detection of urease activity in the oral cavity is considered to be an efficient way to prevent dental caries and also to screen for helicobacter pylori infection. Herein, a rapid surface enhanced Raman scattering (SERS) method is proposed to determine the activity of urease by using inositol hexaphosphate (IP_6) stabilized silver nanoparticles (AgNPs@IP_6) as an efficient SERS-active substrate. The determination was achieved by monitoring the SERS peak intensity of urea at 1003 cm^{-1}. With urease increase, the response of urea at 1003 cm^{-1} decreases gradually, indicating the two has good correlation. A linear relationship between the absolute value of signal drop and urease concentration is observed in a range from 2.35 to 37.5 μg/mL. In addition, the rapid SERS method was used to evaluate the activity of urease in real sample of saliva without any pretreatment, exhibiting a promising potential for biomedical application.

1. Introduction

Urease as nickel-containing enzymes are found in various organisms, including bacteria, fungi, algae, plants and some invertebrates (Karmali et al., 2004). Structurally, ureases from different sources are composed of different types of subunits and exhibit high homology of amino acid sequences (Kaltwasser and Schlegel, 1966; Ngo et al., 1982; Roth, 1971). The physiological role of urease is hydrolyzing urea to produce ammonia (NH_3) and carbon dioxide (CO_2) (Van Slyke, 1927). Routinely, bacterial urease is the mode of pathogenesis for many clinical conditions (Mobley and Hausinger, 1989). It is closely related to the formation of infection stones and contributes to the pathogenesis of pyelonephritis, hepatic encephalopathy, hepatic coma, urinary catheter encrustation, and peptic ulceration. The detection of urease especially in oral cavity, in turn, is used as a diagnostic biomarker to assess early oral and systemic disease (Gomez and Nelson, 2017; Kligler and Gies, 1915).

Various excellent techniques have been available to determine urease activity by monitoring ammonia release, carbon dioxide release, or pH increase. As for the colorimetric methods, the released ammonia by urease can be reacted with phenol-hypochlorite (Weatherburn, 1967) or Nessler reagent to form colored substances (Mobley and Hausinger, 1989). Later, the enzyme assays based on urea coupled with the other enzymes, for example, glutamate dehydrogenase or horseradish peroxidase, have been developed for continuous urease activity assessment. Methods to measure $^{14}CO_2$, releasing from ^{14}C-labeled urea are widely explored and require access to a scintillation counter (NMcDonald et al., 1972). Since urea hydrolysis leads to a pH increase, a pH indicator assay with the presence of phenol red has been developed (Hamilton-Miller and Gargan, 1979; Ruiz-Herrera and Gonzalez, 1969). Additionally, many other methods to determine urease activity, including in-gel detection (Shaik-M et al., 1980), potentiometric sensor, and Fourier transform infrared spectroscopy are also reported in literature (Karmali et al., 2004).

Recently, surface enhanced Raman scattering (SERS), as a sensitive and selective analytical technique (Song et al., 2010), has drawn extensive attention in chemical and biomedical diagnosis (Xu et al., 2014). As well known, SERS effect is dominated by the strong electromagnetic field (Porter et al., 2008), which is attributed to the localized surface Plasmon resonance (LSPR) of some noble metal nanomaterials (Huang et al., 2010). Among them, gold and silver nanoparticles (Au and AgNPs) are the most widely investigated and used for SERS applications (Chen and Liu, 2012). Due to the specific molecular level information it offers, SERS spectroscopy has been applied for enzyme assays. Recently, Cai et al. reported a novel "turn-off" SERS biosensor for the protein arginine kinase McsB detection based on arginine N-phosphorylation (Cai et al., 2018). Besides, other proteins including disease-specific enzyme and protein kinase A were also determined with SERS technique (Maher et al., 2010; He et al., 2018), but there is no report about SERS detection of urease.

In this work, we proposed a facile SERS method for the determination of urease activity by preparing inositol hexaphosphate

* Corresponding authors.
E-mail addresses: yipingwu@shnu.edu.cn (Y. Wu), hfyang@shnu.edu.cn (H. Yang).

https://doi.org/10.1016/j.bios.2018.12.059
Received 11 November 2018; Received in revised form 25 December 2018; Accepted 27 December 2018
Available online 15 January 2019
0956-5663/

encapsulated silver nanoparticles as the active SERS substrate. In this case, urea with a symmetrical chemical structure presents an intense SERS peak at 1003 cm^{-1}. In the presence of urease, urea turns into NH_3 and CO_2, which will both release from the reaction mixture, resulting in a decrease of the SERS signal of urea. Consequently, the SERS signal level of urea is closely relative to the content of urease. In real application, such reaction-based SERS method can be employed to determinate urease activity from oral micro biomes at the community level.

2. Experimental section

2.1. Chemicals and materials

Urea was purchased from Sinopharm Chemical Reagent Co., Ltd. (Shanghai, P. R. China). α-Amylase and lysozyme were bought from Solarbio ((Beijing, P. R. China). Urease, bovine serum albumin (BSA), silver nitrate ($AgNO_3$), sodium citrate, sodium salt of inositol hexaphosphate, inositol hexaphosphate and rhodamine 6G (R6G) were bought from Sigma-Aldrich (St. Louis, MO, USA). The enzyme solution was freshly prepared. All chemicals were used without further purification. All aqueous solutions were prepared with deionized water (18.2 Ω cm), made from the Shanghai senkang Milli-Q system.

2.2. Instruments

Surface Plasmon resonance spectra of the prepared colloids were recorded by a UV–visible spectrophotometer (UV-7504, Shanghai XinMao Instrument Co. Ltd.). The FTIR experiment was conducted with Nicolet iS5 (Thermo Fisher, USA). The transmission electron microscopy (TEM) image of the nanoparticles was measured on a JEOL JEM-2100operating at 200 kV. Raman detection was carried out on a Dilor confocal laser Raman system (Super Lab Ram II) with a 5 mW He-Ne laser at 632.8 nm. The acquisition time was 8 s with 3 accumulations.

2.3. Synthesis of the AgNPs@IP_6

According to the previous work (Xiang et al., 2018; Wang et al., 2010), 25.5 mg of the silver nitrate was dissolved in 150 mL of deionized water in the flask. After the silver nitrate solution was heated to boiling, 5 mL of 10^{-3} M IP_6 solution was added. Keeping 15 min stirring, 3 mL of 1% sodium citrate was slowly added into the boiling solution by drop and drop. The reaction lasted 6 h under the condition of stirring and boiling. As the reaction proceeding, the color of the solution changed from colorless to a light yellow, then orange, brown, finally gray brown. The silver sol was obtained when the solution was cooled down to room temperature and was stored at 4 °C for further use.

2.4. SERS measurement of urea

The stock urea solutions with different concentrations were prepared. Prior to SERS experiments, 10 μL of urea solution was uniformly mixed with 10 μL of $AgNP_S$@IP_6 and incubated at 37 °C for 30 min. After that, 10 μL of the mixture was dropped on a piece of clean aluminum foil and dried at room temperature for SERS measurement.

2.5. SERS tracking urea decomposition catalyzed by urease

10 μL of 0.05 mM urea was first mixed with 10 μL of $AgNP_S$@IP_6. Then, 10 μL of urease solution with different concentrations was added into the mixture. The whole solution was mixed uniformly and kept in the shaking table at 37 °C for another 30 min. After that, 10 μL of the mixture was dropped on a piece of clean aluminum foil and dried at room temperature for SERS measurement.

2.6. Detection of urease in saliva

Saliva sample were obtained from volunteer with informed consent. The detection of urease in saliva was carried out as follow: 90 μL of phosphate buffer solution (10 mM, pH 7.0), 100 μL of 0.05 mM urea and 10 μL of AgNPs@IP_6 aqueous solution were added into a 250 μL tube. Then, a certain amount of saliva was added into the above solution. The resultant mixture was incubated at 37 °C for 30 min. Finally, 10 μL of the mixture was dropped on a piece of clean aluminum foil and dried at room temperature for following SERS measurement.

3. Results and discussion

3.1. Characterization of $AgNP_S$@IP_6

The surface Plasmon resonance (SPR) spectrum of $AgNP_S$@IP_6 was carried out. As shown in Fig. S1, the spectrum presents narrow peak at 413 cm^{-1}, suggesting the successful synthesis of the $AgNP_S$@IP_6 (Wang et al., 2010). Inset of Fig. S1 is the TEM image of $AgNP_S$@IP_6. Clearly, the prepared $AgNP_S$@IP_6 is spherical with a diameter of approximately 30 nm. $AgNP_S$@IP_6 in the image is uniform in size, which is in accordance with the narrow peak of the SPR spectrum. Moreover, the obtained $AgNP_S$@IP_6 shows a high-density AgNPs in IP_6 chain linkage with the structure of hot spots. It enables $AgNP_S$@IP_6 to be suitable for the detection of trace sample with the excellent Raman enhancement effect. The existence of IP_6 on the surface of AgNPs was proved by FTIR. As shown in Fig. S2 and Table S1, the FITR peak at 1126 cm^{-1} in the FTIR spectrum of $AgNP_S$@IP_6 are attributed to the vibration of P-O in PO_3^{2-} (Persson et al., 1996; Arai and Sparks, 2001) Clearly, in comparison of the FTIR spectra of $AgNP_S$@IP_6 and IP_6, both peaks at 1455 and 2922 cm^{-1} are from the IP_6 vibrations in $AgNP_S$@IP_6 (Guan et al., 2006). Therefore, the presence of IP_6 on the surface of AgNPs can be confirmed. (Scheme 1)

3.2. The SERS performance of substrates

Fig. S3 is the concentration dependent Raman spectra of R6G recorded on AgNPs@IP_6 for checking SERS enhancement effect. As the amplified SERS spectrum shown in the inset of Fig. S3, the lowest detectable concentration of R6G can reach 10^{-9} M, suggesting that the synthesized AgNPs@IP_6 has great enhancement effect for Raman scattering. The assignment for the observed SERS peaks of R6G is added in the Supporting information. To further prove the effect of IP_6, the response of R6G with different concentrations were also recorded on the surface of the naked AgNPs. As shown in Fig. S4, in comparison with AgNPs, the noble nanoparticles decorated with IP_6 have a better enhancement effect. According to our previous research, the exits of IP_6 also improve the stability and biological compatibility of AgNPs, which

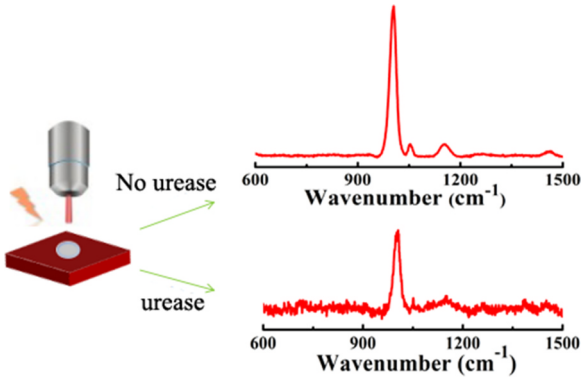

Scheme 1. Schematic diagram of the SERS assay for the determination of urease activity.

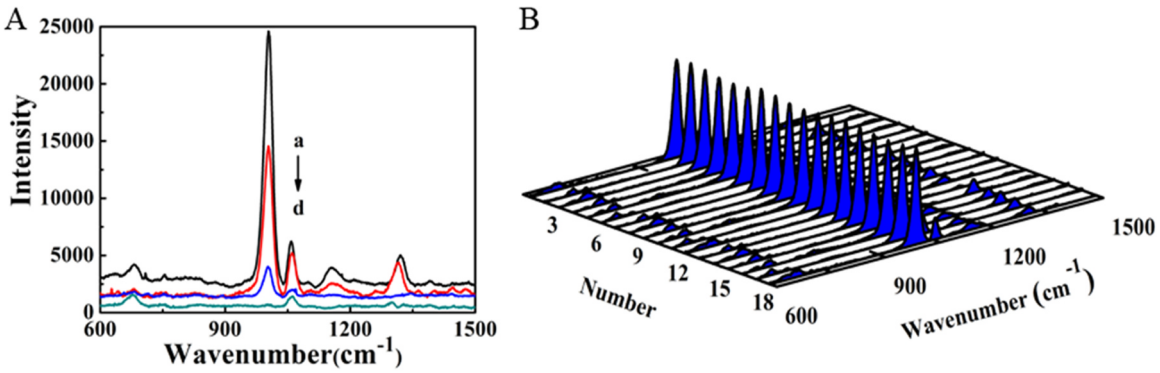

Fig. 1. (A) SERS spectra of urea with different concentrations, from a to d: 5, 0.5, 0.05, 0 mM, recorded on the AgNPs@IP_6 substrate. (B) Raman detection reproducibility by the AgNPs@IP_6 estimated from 18 random acquirement spots (0.5 mM urea).

is beneficial to biological sample detection (Wang et al., 2012; Yang et al., 2015).

3.3. Detection of urea

Fig. 1A shows the SERS spectra of urea with different concentrations on AgNPs@IP_6. As noted above, the characteristic peak of urea is located at 1003 cm^{-1} which is from the N-C-N symmetry stretching mode (Yang et al., 2018). Clearly, the usage of urea at 0.5 mM contributes the greatest Raman signal. For evaluating the reproducibility of AgNPs@IP_6, SERS spectra of urea on the AgNPs@IP_6 were recorded from 18 randomly sampling spots. As observed in Fig. 1B, the relative standard deviation (RSD) is 2.71%, demonstrating the good reproducibility of Raman detection by using the AgNPs@IP_6. It is helpful to the next quantitative analysis of enzyme activity.

As mentioned above, the intensity of the peak at 1003 cm^{-1} declines with the removal of urea by urease, which could be the indication of enzyme activity. To explore the feasibility of SERS determining the urease activity, the AgNPs@IP_6-based SERS spectra of pure urea, pure urease and urea with urease are first recorded. Compared with the SERS spectrum of pure urea (Fig. 2A (a)), the SERS band intensity of urea at 1003 cm^{-1} in Fig. 2A (b) drops off after incubation with certain concentration of urease, while urease has no SERS response on the surface of AgNPs@IP_6 (Fig. 2A (c)). As a big bimolecular, urease might cover the AgNPs@IP_6 surface and be a barrier around AgNPs@IP_6 for urea approaching. This can also lead to a drop in urea Raman signal. Therefore, a control experiment is conducted to investigate the role of urease. In detail, the similar SERS spectra of R6G on AgNPs@IP_6 acquired with and without urease clearly show that Raman response of R6G on AgNPs@IP_6 is not affected by the presence of urease (Fig. 2B). This, in turn, suggests that the drop in urea Raman signal is due to the breakdown of urea by urease.

Urease concentration dependent SERS spectra of urea are shown in Fig. 3A. Obviously, the peak intensity of urea decreases progressively with the successive addition of urease. Taking the SERS intensity of 0.5 mM urea at 1003 cm^{-1} as the original intensity, the value of signal drop is estimated by subtracting the Raman intensity of urea without urease from that of urea with urease. Fig. 3B is a plot of the signal drop value as a function to urease concentration, which exhibits a linear range from 2.35 to 37.5 μg/mL (R^2 = 0.998). Compared with the other methods (Mobley and Hausinger, 1989), the urea-based SERS probe for evaluation of enzyme activity is quite easy and no extra reagent is needed. The above observation demonstrates that the developed reaction-based SERS method can be used to determine the activity of urease.

To correctly identify the activity of urease, good selectivity is required for the method. The selectivity of the assay was evaluated in the following experiment. BSA and the other two common proteins in saliva including α-amylase and lysozyme were selected for the interference test. In Fig. 4A, the Raman signals of urea incubated with urease

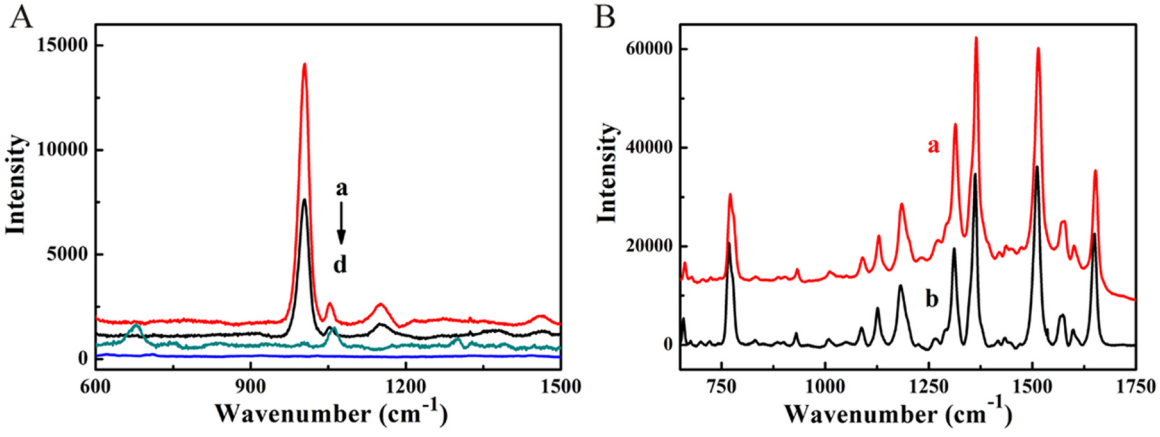

Fig. 2. (A) SERS spectra of (a) 0.5 mM urea, (b) 0.5 mM urea after it was incubated with 9.40 μg/mL of urease at 37 °C for 30 min, (c) 0.60 mg/mL urease, (d) AgNPs@IP_6. (B) SERS spectra of (a) 10^{-6} M R6G on AgNPs@IP_6, (b) 10^{-6} M R6G on AgNPs@IP_6 which was previously incubated with 0.60 mg/mL of urease at 37 °C for 30 min.

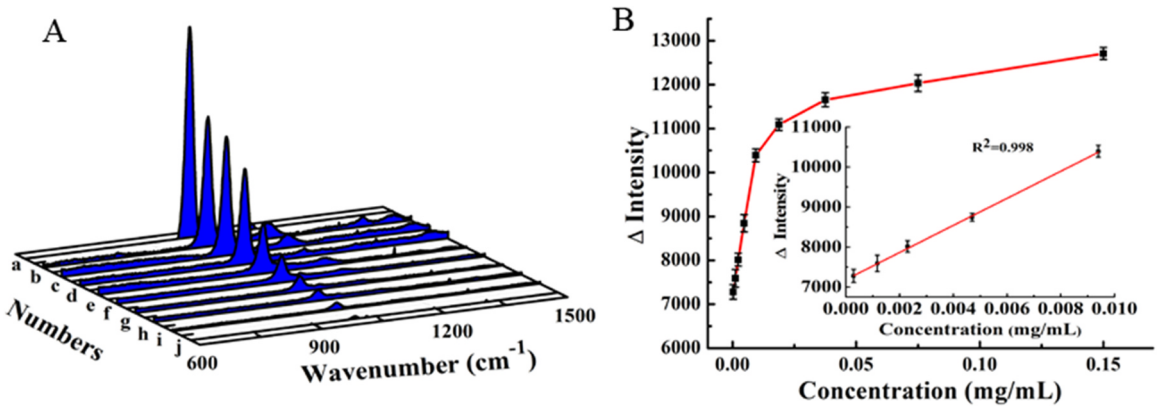

Fig. 3. (A) SERS spectra of 0.5 mM urea after it was incubated with different concentrations of urease at 37 °C for 30 min. From a to j: 0, 2.35, 4.70, 9.40, 18.8, 37.5 μg/mL, 0.075, 0.15, 0.30, 0.60 mg/mL urease. (B) The decrease of SERS intensities at the band of 1003 cm^{-1} as a function of urease concentration. Inset is the linear relationship range. The error bar represents the standard deviation of 3 replicate measurements.

decrease sharply, while that of urea incubated whether with BSA, α-amylase or lysozyme, have no significant change. In organisms, urease with various species is specific responsible for the hydrolysis of urea. Co-existing proteins such as BSA herein as a transporter protein and α-amylase or lysozyme as an effective enzyme to starch and peptidoglycan respectively is not expected to hydrolyze urea and effect the specific enzyme-based reaction (Dou et al., 1997; He et al., 2018).

3.4. Detection of urease in saliva

To apply the urea-reaction-based SERS assay for biomedical detection, we determine the urease activity in saliva. As above-stated, oral bacteria is closely related with human health (Gomez and Nelson, 2017). In detail, the detection of urease activity in the oral cavity is considered to be an efficient way to prevent dental caries and screen for helicobacter pylori infection (Zhang et al., 2017; Payão and Rasmussen, 2016; Lee et al., 2000). As shown in Fig. 4B, the SERS spectra of urea in saliva spiked with two concentrations of urease, involving 4.70 and 9.40 μg/mL, was obtained. With the dilution, saliva itself has no SERS response on the substrate. As the amount of urease increases, the SERS intensity of urea at 1003 cm^{-1} in saliva decreases. The recoveries were found in the range of 99.9–101% with the RSD values less than 5% (listed in Table 1), confirming that the proposed SERS method is a rapid and effective technique for monitoring urease activity in saliva.

Table 1
Recoveries for determination of urease in diluted saliva samples.

Sample	Added (μg/mL)	Found (μg/mL)	Recovery n = 3 (%)	RSD n = 3 (%)
1	4.70	4.77	101	5.19
2	9.40	9.39	99.9	3.01

4. Conclusion

In summary, a cost-effective SERS method based on a high SERS-active substrate of AgNPs@IP_6 was developed for determining the activity of ureas in saliva without any pretreatment. By monitoring the SERS peak intensity of urea, the method can detect as low as 2.35 μg/mL urease. Besides, the method has high selectivity because of the involved specific enzymic-catalytic reaction between urea and urease. Combined with a portable Raman spectrum, the SERS assay has great potential for urease detection in biomedical diagnosis and can provide improved assessment in individuals and populations at risk.

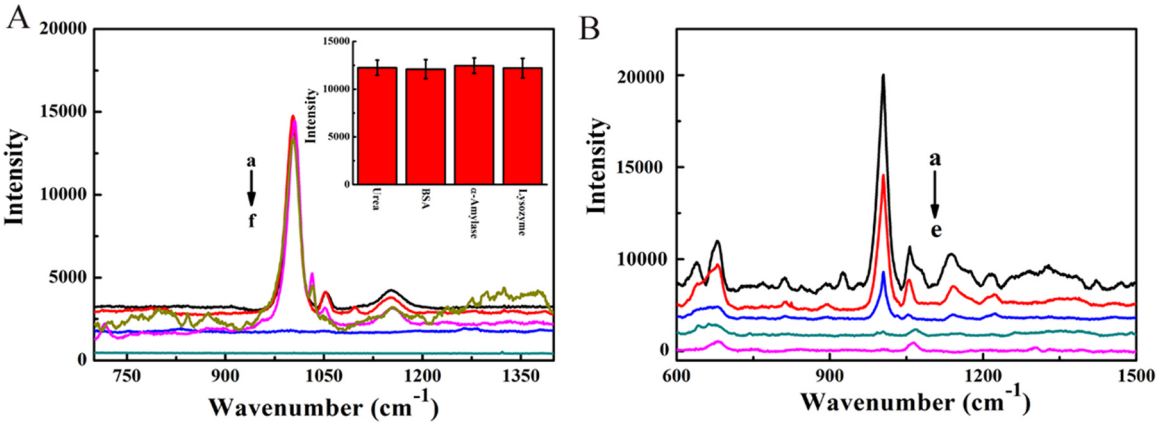

Fig. 4. (A) SERS spectra of (a) 0.5 mM urea, (b, c, d, e) 0.5 mM urea after it was incubated with 0.6 mg/mL BSA, α-amylase, lysozyme, urease at 37 °C for 30 min, respectively, (f) AgNPs@IP_6. Inset is the histogram of a, b, c, d. (B) SERS spectra of (a) 0.05 mM urea in saliva, (b, c) 0.05 mM urea after it was incubated with 4.70 and 9.40 μg/mL urease in saliva at 37 °C for 30 min, (d) saliva, (e) AgNPs@IP_6.

Acknowledgements

This work is supported by the National Natural Science Foundation of China (21475088, 21507087), PCSIRT (IRT1269), Shanghai Government (18DZ2254200), Chenguang Program of Shanghai Municipal Education Commission, International Joint Laboratory on Resource Chemistry (IJLRC) and Shanghai Key Laboratory of Rare Earth Functional Materials.

Supporting information

The Supporting information is available free of charge. It includes the UV–vis spectrum and TEM image of AgNPs@IP_6, FTIR spectra of IP_6 and the assignments, the SERS spectra of R6G with different concentrations recorded on the substrate of AgNPs@IP_6 and AgNPs, and the Raman spectrum of bulk urea.

Declaration of interests

None.

Credit author statement

Sen Hu did all the experiments and wrote the original draft.
Yun Gao helped to process the data with the software.
Yiping Wu provided the conceptualization and edit the draft.
Xiaoyu Guo helped to review the draft.
Ye Ying helped to review the draft.
Ying Wen helped to review the draft.
Haifeng Yang supervised the whole work, including the experiments, the data and the draft.

Appendix A. Supporting information

Supplementary data associated with this article can be found in the online version at doi:10.1016/j.bios.2018.12.059.

References

Arai, Y., Sparks, D.L., 2001. J. Colloid Interface Sci. 241, 317.
Chen, L.M., Liu, Y.N., 2012. J. Raman Spectrosc. 43, 986–991.
Cai, H., Huang, B., Lin, R., Xu, P., Liu, Y., Zhao, Y., 2018. Talanta 189, 353–358.
Dou, X., Takama, T., Yamaguchi, Y., Yamamoto, H., 1997. Anal. Chem. 69, 1492–1495.
Gomez, A., Nelson, K.E., 2017. Microb. Ecol. 73, 492–503.
Guan, X., Shang, C., Zhu, J., Chen, G., 2006. J. Colloid Interface Sci. 293, 296–302.
Hamilton-Miller, J.M.T., Gargan, R.A., 1979. Urol 16, 327–328.
He, S., Kyaw, Y.M.E., Tan, E.K.M., Bekale, L., Kang, M.W., Cherng, Susana Kim, S.Y., Tan, I., Peng, L.K., 2018. Anal. Chem. 90, 6071–6080.
Huang, Y.F., Yin, N.N., Wang, X., Wu, D.Y., Ren, B., Tian, Z.Q., 2010. Chem. Eur. J. 16, 1449–1453.
Kaltwasser, H., Schlegel, H.G., 1966. Anal. Biochem. 16, 132–138.
Karmali, K., Karmali, A., Teixeira, A., Marcelo Curtob, M.J., 2004. Anal. Biochem. 331, 115–121.
Kligler, I.J., Gies, W.J., 1915. J. Allied Dent. Soc. 10, 445–458.
Lee, J.M., Breslin, N.P., OMorain, C.A., 2000. Am. J. Gastroenterol. 95, 1166.
Maher, R.C., Maier, S.A., Cohen, M.M., 2010. J. Phys. Chem. C 114, 7231–7235.
Mobley, H.T., Hausinger, R.P., 1989. Microbiol. Rev. 53, 85–108.
Ngo, T.T., Phan, A.P.H., Yam, C.F., Lenhoff, H.M., 1982. Anal. Chem. 54, 46–49.
NMcDonald, J.A., Speeg Jr., K.V., Campbell, J.W., 1972. Enzymologia 42, 1–9.
Payão, S.L.M., Rasmussen, L.T., 2016. World J. Gastrointest. Pharmacol. Ther. 7, 126–132.
Persson, P., Nilsson, N., Sjöberg, S., 1996. J. Colloid Interface Sci. 177, 263.
Porter, M.D., Lipert, R.J., Siperko, L.M., Wang, G.F., Narayanan, R., 2008. Chem. Soc. Rev. 37, 1001–1011.
Roth, M., 1971. Anal. Chem. 43, 880–882.
Ruiz-Herrera, J., Gonzalez, J., 1969. Anal. Biochem. 31, 366–374.
Shaik-M, M.B., Guy, A.L., Pancholy, S.K., 1980. Anal. Biochem. 103, 140–143.
Song, S.P., Qin, Y., He, Y., Huang, Q., Fan, C.H., Chen, H.Y., 2010. Chem. Soc. Rev. 39, 4234–4243.
Van Slyke, D.D., 1927. J. Biol. Chem. 73, 695–723.
Wang, N., Wen, Y., Wang, Y., Zhang, R., Zhang, X.Y., Xiong, D.H., Yang, H.F., 2010. J. Mater. Chem. 20, 2317–2321.
Wang, N., Wen, Y., Wang, Y., Zhang, R., Chen, X., Ling, B., Huan, S., Yang, H.F., 2012. Nanotechnology 23, 145702.
Weatherburn, M.W., 1967. Anal. Chem. 39, 971–974.
Xiang, Y., Li, M.H., Guo, X.Y., Wu, Y.P., Ying, Y., Wen, Y., Yang, H.F., 2018. Sens. Actuators B Chem. 262, 44–49.
Xu, J.J., Zhao, W.W., Song, S.P., Fan, C.H., Chen, H.Y., 2014. Chem. Soc. Rev. 43, 1601–1611.
Yang, H.R., Xiang, Y., Guo, X.Y., Ying, Y.P., Wen, Y., Yang, H. F, Y., 2018. Sens. Actuators B Chem. 271, 118–121.
Yang, T.X., Guo, X.Y., Wang, H., Fu, S.Y., Wen, Y., 2015. Biosens. Bioelectron. 68, 350–357.
Zhang, X.Y., Zhang, P.Y., Aboul-Soud, M.A.M., 2017. Oncol. Lett. 13, 543–548.